mathematics

Article

Optimal Operation of PV Sources in DC Grids for Improving Technical, Economical, and Environmental Conditions by Using Vortex Search Algorithm and a Matrix Hourly Power Flow

Luis Fernando Grisales-Noreña [1,*], Andrés Alfonso Rosales-Muñoz [2], Brandon Cortés-Caicedo [2], Oscar Danilo Montoya [3,4] and Fabio Andrade [5]

1 Department of Electrical Engineering, Faculty of Engineering, Universidad de Talca, Curicó 3340000, Chile
2 Departamento de Mecatrónica y Electromecánica, Facultad de Ingeniería, Instituto Tecnológico Metropolitano, Medellín 050036, Colombia
3 Grupo de Compatibilidad e Interferencia Electromagnética (GCEM), Facultad de Ingeniería, Universidad Distrital Francisco José de Caldas, Bogotá 110231, Colombia
4 Laboratorio Inteligente de Energía, Facultad de Ingeniería, Universidad Tecnológica de Bolívar, Cartagena 131001, Colombia
5 Electrical and Computer Engineering Department, University of Puerto Rico at Mayaguez, Mayaguez, PR 00680, USA
* Correspondence: luis.grisales@utalca.cl

Abstract: This document presents a master–slave methodology for solving the problem of optimal operation of photovoltaic (PV) distributed generators (DGs) in direct current (DC) networks. This problem was modeled using a nonlinear programming model (NLP) that considers the minimization of three different objective functions in a daily operation of the system. The first one corresponds to the minimization of the total operational cost of the system, including the energy purchasing cost to the conventional generators and maintenance costs of the PV sources; the second objective function corresponds to the reduction of the energy losses associated with the transport of energy in the network, and the third objective function is related to the minimization of the total emissions of CO_2 by the conventional generators installed on the DC grid. The minimization of these objective functions is achieved by using a master–slave optimization approach through the application of the Vortex Search algorithm combined with a matrix hourly power flow. To evaluate the effectiveness and robustness of the proposed approach, two test scenarios were used, which correspond to a grid-connected and a standalone network located in two different regions of Colombia. The grid-connected system emulates the behavior of the solar resource and power demand of the city of Medellín-Antioquia, and the standalone network corresponds to an adaptation of the generation and demand curves for the municipality of Capurganá-Choco. A numerical comparison was performed with four optimization methodologies reported in the literature: particle swarm optimization, multiverse optimizer, crow search algorithm, and salp swarm algorithm. The results obtained demonstrate that the proposed optimization approach achieved excellent solutions in terms of response quality, repeatability, and processing times.

Keywords: direct current networks; grid-connected network; standalone network; metaheuristic optimization methods; master–slave methodology; photovoltaic generation; minimization of operating costs; minimization of energy losses; minimization of CO_2 emissions

MSC: 65K05; 90C26; 90C27

check for updates

Citation: Grisales-Noreña, L.F.; Rosales-Muñoz, A.A.; Cortés-Caicedo, B.; Montoya, O.D.; Andrade, F. Optimal Operation of PV Sources in DC Grids for Improving Technical, Economical, and Environmental Conditions by Using Vortex Search Algorithm and a Matrix Hourly Power Flow. *Mathematics* **2023**, *11*, 93. https://doi.org/10.3390/math11010093

Academic Editors: Kuo Tian, Weizhu Yang and Shiyao Lin

Received: 24 November 2022
Revised: 12 December 2022
Accepted: 19 December 2022
Published: 26 December 2022

Copyright: © 2022 by the authors. Licensee MDPI, Basel, Switzerland. This article is an open access article distributed under the terms and conditions of the Creative Commons Attribution (CC BY) license (https://creativecommons.org/licenses/by/4.0/).

1. Introduction

1.1. General Context

These days, it is possible to appreciate how electrical energy has become a fundamental basis for the development of human societies, increasing the consumption of electrical

energy worldwide [1–3]. Accordingly, power generation plants (mainly thermal power plants) increase their dependence on fossil fuels to meet growing demand, by increasing the emission of polluting gases and negatively impacting the environment [4,5]. To mitigate this problem, different governmental entities around the world have promoted the development and implementation of technologies based on renewable energy sources and energy storage systems (i.e., distributed energy resources). Likewise, the inclusion of these devices has been facilitated by the fact that construction and production costs have decreased in recent years due to the different technological advances in power electronics [6,7].

As a result of these technological advances, the implementation of direct current (DC) networks is now a viable alternative at the transmission and sub-transmission stages to meet the demand of end users (i.e., residential, industrial, and commercial) at medium and low voltage levels. Thus, the advantages of DC networks over traditional AC networks are as follows [8,9]: (i) higher efficiency, since the absence of reactive elements (i.e., inductive reactance and reactive power flows) reduces power losses and improves voltage profiles; (ii) reduction of operating and investment costs associated with network maintenance; and (iii) simple integration of distributed energy resources into the network, as most of them operate in DC. For the last reasons, the implementation of technologies based on renewable resources, such as solar photovoltaic (PV) and wind power generation systems, has been growing in recent years, in addition to the fact that their zero-emission operation makes them a viable opportunity for the global energy transition [10].

1.2. Motivation

The Colombian case is no stranger to this situation; in recent years, through regulations and legislation such as Law 1715 of 2014, CREG 030 of 2018, and 068 of 2020, the development of large-scale projects related to the integration and operation of photovoltaic (PV) generation sources within conventional grids has been promoted [11]. This growing interest is related to its geographical location and the abundant solar resource that is currently far from being fully exploited [11,12]. Additionally, analyzing the country's energy matrix, it is possible to observe that 69.4% of the country's electricity is generated from renewable energy sources (hydroelectric, solar, and wind, among others), where less than 0.76% is generated from solar resources. However, approximately 30.7% of electricity is generated from fossil fuels, such as coal (9.6%), diesel (7.8%), and natural gas (13.3%), which contribute significantly to the emission of CO_2 into the atmosphere [13]; this generates an exceptional scenario for the inclusion of renewable energies.

For the last reasons, the main motivation of this research is to propose an optimization methodology that allows taking advantage of the abundant solar resource existing in Colombia. Thus, it is expected that through the correct operation of distributed PV generators located along grid-connected or standalone DC distribution, the technical (reduction of energy losses), economical (reduction of operating costs), and environmental (reduction of CO_2 emissions) conditions will be improved. Furthermore, this research also aims to propose solutions that will allow a country such as Colombia to achieve an energy transition that reduces emissions of polluting gases while providing a high-quality service, as economically as possible, to all users located in both grid-connected and standalone networks.

1.3. State of the Art

In recent years, in the specialized literature, different works have been reported related to operation of PV DGs in DC distribution networks. This problem can be oriented towards meeting technical, economical, or environmental criteria. Some of these works are presented below.

In [14], the economical dispatch problem was formulated with the objective of minimizing the total cost operation in a DC grid. This cost was associated with conventional and renewable-energy-based generators (e.g., PV and wind generators), and the cost efficiency of the system, by considering the demand response requirements. This solution was tested

in a six-node test system using the genetic algorithm as optimization methodology, demonstrating that, under a variable renewable energy scenario, the proposed methodology reduces the operating costs by an important percent without using comparison methods and processing time analysis. In [15], a new methodology was presented to evaluate the technoeconomical feasibility of the integration and operation of large-scale PV generators in AC/DC distribution networks, whereby the objective functions considered were the minimization of operating costs and power losses. The nondominant sorting genetic algorithm-II was used to solve this problem. The numerical results were obtained in the 33 bus test, a grid-connected electrical system with grid-connected conditions, demonstrating the feasibility of the proposed methodology. The authors of [16] presented an optimal dispatch model for the operation of a generation system composed of wind, PV, and thermal energy sources. In this paper, the dispatch could be performed in five different ways in order to minimize the generation costs, while at the same time reducing the emissions of polluting gases. This model was applied to a real DC system located in Tianzhong-Xinjiang, China, where it was found that it is possible to maximize the energy generated from the energy sources by reducing the environmental impact of the grid operation. In [17], the authors proposed the memory-based gravitational search algorithm for minimizing energy generation costs in a DC grid. The authors employed the 37 bus IEEE test system to optimize the power generation from different types of generation, such as PV systems, cogeneration systems, and diesel generators. The results obtained in this work showed that the proposed methodology presented a better performance to solve the addressed problem in comparison with other metaheuristic algorithms, such as artificial bee colony, genetic algorithm, and particle swarm optimization. They demonstrated the effectiveness of the proposed methodology without analyzing the processing time required for the solution methods used.

The authors of [8] presented a second-order conic programming model to solve the optimal dispatch problem of distributed generators in DC grids. The objective of this work was the minimization of power losses for DC systems in a single hour of operation. This methodology was applied in different test systems with radial and meshed topology, where the numerical results were compared with two metaheuristic methods, demonstrating the efficiency and robustness of the proposed methodology. In references [18,19], a master–slave methodology was presented to solve the problem of optimal dispatch of distributed generation sources in DC networks. These research papers aimed at minimizing system power losses. In both works, they analyzed the repeatability and quality of the solution obtained by the solution methodologies proposed, with consideration of the processing times required for these. In [18], the black hole optimization was used in conjunction with the classical Gauss–Seidel power flow method for solving the problem of optimal power dispatch in DC grids, to reduce the power losses, while in [19], the authors used the Ant Lion Optimizer in conjunction with the successive approximations method. Both papers demonstrated the efficiency and robustness of the proposed methodologies by solving the problem posed on the 21 bus and 69 bus test systems. The authors of [20] proposed a hybrid methodology between the particle swarm optimization algorithm and the gravitational search algorithm for solving the integration and dispatch problem of renewable energy sources based mainly on PV and wind generation in DC grids. The main objective of this paper was to minimize the energy losses of the grid and maximize the profit of the owners of renewable energy sources, by avoiding the implementation of commercial software. Numerical results were derived on the 69 bus test system, demonstrating the efficiency and applicability of the proposed methodology, in terms of solution quality and processing times, compared to other population-based metaheuristic algorithms. Finally, in reference [21], a mixed-integer nonlinear programming model for the integration and operation of PV generators in DC networks was presented. Variable generation and demand curves were considered in this paper. The objective of this paper was to minimize the total CO_2 emissions produced by diesel generators in isolated areas. This model was

solved using GAMS software. Numerical results on the 21-node test system demonstrated the applicability and effectiveness of the proposed methodology.

By analyzing the state-of-the-art works presented, it is possible to notice that the main characteristics of the optimization methodologies reviewed are the following: (i) most of the reported methodologies focus on minimizing operating costs, reduction of power or energy losses, and, finally, to minimize the pollutant gas emissions; (ii) there is no evidence of solution strategies that evaluated the effects for improving all conditions, such as technical, economical, and environmental, to give grid operators the possibility to select and optimize one of these conditions according to their policies and needs; (iii) not all of the technical–operational restrictions that represent the operation of a DC distribution system under a PV generation environment are considered, and it is important to know and respect the thermal limits of the existing conductors in the network when operating PV systems; (iv) for calculating the values of the objective functions, in the operation of PV generators, the maximum power point is used, which forces these generators to generate the maximum power available in all periods of time, which can affect the stability of the grid in case the power generated with the solar resource exceeds the power demanded by the users. Finally, it is identified that there is a need to evaluate the performance of the solution methodologies proposed by analyzing the average solution, standard deviation, and processing times, with the aim of guaranteeing that each time the proposed methodology is executed, there is a solution of good quality in terms of solution, repeatability, and processing times. This kind of analysis is widely used in the literature to evaluate the effectiveness of proposed solutions to power flow problems in electrical systems [22,23].

1.4. Scope and Main Contributions

This document proposes the implementation of a master–slave methodology with the primary objective of improving the technical, economical, and environmental conditions associated with the daily operation of electrical DC distribution networks. Considering the review of the state of the art presented above, the main contributions of this paper are listed below:

i. A new master–slave approach to solve the NLP model that represents the problem under study in grid-connected and standalone DC networks. The master stage uses the Vortex Search algorithm (VSA) with a continuous codification to define the output power of the PV distributed generators without obliging the electrical system to follow the maximum power point every time. This allows a flexible power injection by the PV DGs.
ii. In the slave stage, a matrix successive approximation power flow method is proposed to evaluate the objective functions proposed and the constraints that comprise the problem, by considering an variable power generation and demand scenario. This matrix formulation of power flow guarantees the convergence of the solution and reduces the processing time required when compared with a classical hourly power flow reported in the literature.
iii. A methodology that presents the best trade-off between the quality solution and processing times when analyzing economical, technical, and environmental indexes in DC grids.
iv. Two grid-connected and standalone test systems based on the operative conditions of Colombian regions.

1.5. Paper Organization

This document is structured as follows: Section 2 presents the mathematical formulation that represents the problem of optimal operation of PV distributed generation units in DC distribution networks considering different objective functions. Section 3 describes the implementation of the proposed master–slave methodology that integrates the VSA with the proposed matrix hourly power flow method based on successive approximation. Section 4 presents the main characteristics of the 33 bus test system for the grid-connected

case and the 27 bus test system for the standalone case, the typical PV generation and demand curve for both test feeders, and the parametric information required to calculate the value of the economical, technical, and environmental conditions. Section 5 shows the numerical results, validations, analysis, and discussion regarding the optimal operation of PV distributed generation units for both DC test systems. Finally, Section 6 lists the main conclusions and future works derived from this research.

2. Mathematical Formulation

In this section, we present the mathematical formulation of the problem of optimal operation of PV DGs in DC grids for improving the economical, technical, and environmental conditions in grid-connected and standalone networks, by considering variable power generation and demand for a day of operation (24 h in intervals of one hour).

$$\min\ E_{cost} = f_1 + f_2, \tag{1}$$

$$f_1 = C_{kWh}\left(\sum_{h\in\mathcal{H}}\sum_{i\in\mathcal{N}} p^{s}_{i,h}\Delta h\right), \tag{2}$$

$$f_2 = C_{O\&M}\left(\sum_{h\in\mathcal{H}}\sum_{i\in\mathcal{N}} p^{pv}_{i,h}\Delta h\right), \tag{3}$$

Equation (1) presents the objective function related to the reduction of operational costs of the grid E_{cost}. This equation is composed of the energy purchasing cost of the conventional generators located in the DC grid (f_1), and the maintenance costs of PV distributed generators (f_2). For calculating f_1, we use Equation (2), in which C_{kWh} is the energy purchasing costs per kW in USD, $p^{s}_{i,h}$ is the power supplied by the conventional generator located in the bus i in the hour h, and Δh is the duration of the period of time analyzed; in this particular case, one hour. $\mathcal{H}$ and $\mathcal{N}$ are the set that contain the total number of hours considered in the horizon time (24 h) and buses that make up the DC grid. To calculate f_1, we use Equation (2). In this equation, $C_{O\&M}$ corresponds to the PV maintenance cost in USD per kW produced, while $p^{pv}_{i,h}$ is the power produced by the PV distributed generator located in the bus i in the hour h.

$$\min\ E_{loss} = \sum_{h\in\mathcal{H}}\sum_{l\in\mathcal{L}} R_l I_l^2 \Delta h, \tag{4}$$

Equation (4) describes the objective function related to improving the technical conditions of the grid, by considering, in this particular case, the reduction of energy loss associated with the energy transport in the electrical network (E_{loss}). In this equation, R_l and I_l represent the resistance and flow current of the l branch that belong to the set of branches that comprise the DC grid ($\mathcal{L}$).

$$\min\ E_{CO_2} = CE_s\left(\sum_{h\in\mathcal{H}}\sum_{i\in\mathcal{N}} p^{s}_{i,h}\Delta h\right), \tag{5}$$

Equation (5) is responsible for reducing the CO_2 emission related to the energy production in the DC grid by the conventional generators E_{CO_2}, where CE_s denotes the coefficient of emission of the conventional generators; in the particular case of grid-connected networks, this coefficient is supplied by the grid operator, while in standalone grids, it is associated with the fossil energy resource used.

$$p^{s}_{i,h} + p^{pv}_{i,h} - P^{d}_{i,h} = v_{i,h}\sum_{j\in\mathcal{N}} G_{ij} v_{j,h} \tag{6}$$

$$P^{s,\min}_{i} \le p^{s}_{i,h} \le P^{s,\max}_{i} \tag{7}$$

$$P^{pv,\min}_{i} \le p^{pv}_{i,h} \le P^{pv,\max}_{i} \tag{8}$$

$$P_i^{pv,\max} \leq P_i^{pv} C_h^{pv} \tag{9}$$

$$V_i^{\min} \leq v_{i,h} \leq V_i^{\max} \tag{10}$$

$$-I_l^{\max} \leq I_{l,h} \leq I_l^{\max} \tag{11}$$

The set of technical and operation constraints that represent the problem are illustrated by Equations (6)–(11). Equation (6) is related to the power balance of the grid. In this equation, $P_{i,h}^{d}$ and $v_{i,h}$ are the power demanded and the bus voltage profile in the bus i at the hour h, while G_{ij} is associated with the conductance of the branch connected between the buses i and j, and $v_{j,h}$ is the bus voltage profile in the bus j at the hour h. Equation (7) represents the power limits of the conventional generator located in bus i. In this equation, $P_i^{s,\min}$ and $P_i^{s,\max}$ denote the minimum and maximum limits. In the same way, Equation (8) is associated with the power bound of PV distributed generators; in this equation, $P_i^{pv,\min}$ and $P_i^{pv,\max}$ correspond to the maximum and minimum power to be supplied by the PV distributed generator located at bus i. Here, $P_i^{pv,\min}$ takes a value of 0 kW, while $P_i^{pv,\max}$ is calculated using Equation (9), which is a function of the nominal power of the PV distributed generator located in the bus i and the power capacity of PV system in the hour h; this value is related to the solar radiance, environmental temperature, and PV technology used (see Section 4). Finally, Equations (10) and (11) present the operative constraints associated with the voltage and branch current. The first equation guarantees that the DC grids operate between the maximum ($V_i^{\max}$) and minimum ($V_i^{\min}$) voltage profile allowed, while the second one establishes that the current that circulates on the branch l at the hour h ($I_{l,h}$) must be smaller than the maximum current allowed in this branch I_l max in both flow directions (+ or −).

$$FF = OF + \alpha \begin{pmatrix} \max\{0, V_{i,h} - V_i^{\max}\} \\ -\min\{0, V_{i,h} - V_i^{\min}\} \\ -\min\left\{0, \text{real}(p_{i,h}^{s} - P_i^{s,\min})\right\} \\ +\min\left\{0, \text{real}(p_{i,h}^{s} - P_i^{s,\min})\right\} \\ +\max\{0, I_{l,h} - I_l^{\max}\} \end{pmatrix} \tag{12}$$

To guarantee all constraints that comprise the problem studied here, we used the fitness function (FF) presented in Equation (12). It is important to mention that a fitness function is a common adaptation of the objective function used when working with metaheuristic techniques and should be evaluated using the constraints for each individual proposed by the master stage [24,25]. The implementation of a fitness function (instead of the original objective function) allows efficient exploration and exploitation of the solution space by the algorithm, since exploring not-feasible regions increases the chances of finding a solution of good quality, by reducing processing times in the majority of the cases [26,27].

In this work, this equation considers the penalization of the objective function if any constraint is violated, by comparing the maximum and minimum values allowed with the values generated for the different solutions proposed by the solution method. It is worth clarifying that the objective function in this research paper could be the economical, technical, or environmental condition of the grid, depending on the needs of the network operator. When the solution obtained by an individual is feasible and within the solution space, the original objective function and the adaptation function reach the same numerical value, otherwise penalty factors will be applied to the original objective function to worsen the quality of the response. Finally, with the aim of normalizing the penalization values in relation to the objective functions used, and penalizing the solutions that violate the set of constraints inside the iterative process, the constant α was employed, which, in this particular case, takes a value of 1000 fixed in a heuristic way. This value allows the VSA to explore not-feasible regions, guaranteeing that at the end of the iterative process a feasible solution of good quality will be obtained.

3. Codification and Optimization Methodology

This section describes the codification and solution methodology proposed for solving the problem of optimal dispatch of PV generators in DC grids for improving economical, technical, and environmental indexes.

3.1. Codification Problem

The codification proposed for the problem of optimal operation of PV DGs in DC grids, by considering variable power generation related to the PV technology, solar radiation, and environmental temperature of the region where the PV systems are located, is illustrated in Figure 1. This codification uses a vector of size $1xC$, where $C = SRH * N_{pv}$, and SRH and N_{pv} correspond to the number of solar radiation hours present in the region where the electrical systems are located, and the total of PV DGs installed on the grid. The example shown in Figure 1 is related to PV systems located in Colombian regions, where the SRH is equal to 13 h. This value is obtained with the sun total hours within the horizon time generated from 6 to 19 h, respectively, by generating for 3 PV distributed generators installed on DC grids a total of 39 variables for the codification of the problem. In an example model, in this figure, for the PV distributed generator 1, we consider the injection of 0, 0.3, 1.1, and 0.7 kW at the hours 6, 7, 18, and 19. In the case of the PV distributed generator 2, we propose a power supply of 0.1, 0.4, 1.2, and 0.95 kW at the hours 6, 7, 18, and 19, respectively. Finally, for the PV distributed generator 3, we consider a power of 0, 0.5, 1, and 0.8 kW at the hours 6, 7, 18, and 19. This power configuration represents a possible solution for the problem studied here, with the values generated between the maximum and minimum power allowed for the PV DGs located in the grid, which are calculated by using the PV technology, nominal power, solar radiation, and environmental temperature (see Section 4).

PV Distributed generator 1					PV Distributed generator 2					PV Distributed generator 3				
h=6	h=7	.....	h=18	h=19	h=6	h=7	.....	h=18	h=19	h=6	h=7	.....	h=18	h=19
0	0.3	.....	1.1	0.7	0.1	0.4	.....	1.2	0.95	0	0.5	.....	1	0.8

Figure 1. Codification used for solving the problem of optimal operation of PV DGs in DC grids.

3.2. Solution Methodology

The aim is to find the power values for the codification proposed that allow to obtain the best possible solution for solving the problem of optimal operation of PV distributed generators in DC grids by considering the economical, technical, and environmental indexes reported in Section 2. In this paper, we consider a master–slave strategy as a solution. In the master stage, we use the Vortex Search algorithm (VSA) entrusted to find the power values to be injected by each distributed generator by using the codification described in the last paragraph. In the slave stage, we propose a matrix hourly power flow (MHPF) responsible for calculating the effect of the power values provided by each solution proposed by the VSA from the technical, economical, and environmental points of view, by considering all constraints that represent the problem. Figure 2 describes the dynamic between the master–slave strategy, where the arrow green identifies the sending of solution information, while the red arrow represents the fitness function received by the VSA from the MHPF.

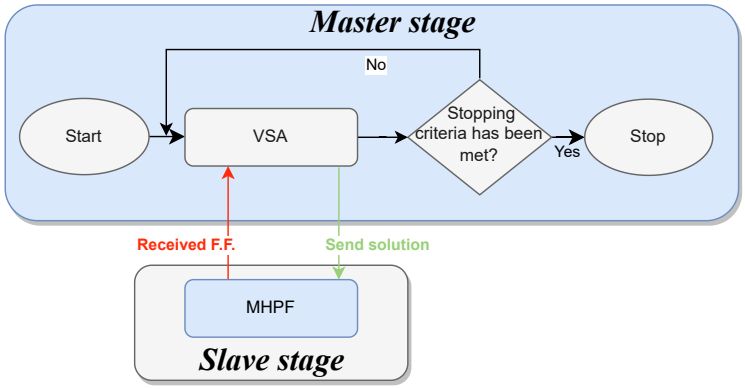

Figure 2. Master–slave methodology proposed.

3.2.1. Vortex Search Algorithm

The VSA is inspired by the vertical behavior of stirred fluids [28], which explore the solution space, spreading the individuals of a population within the solution space through a Gaussian distribution that guarantees an adequate exploration from the mathematical point of view. As the iterative process of the algorithm advances, the diameter size is reduced, changing the center of this to a function of the best solution, with the aim to converge in the best possible solution. The selection of this optimization algorithm was based on the excellent results reported in the literature for solving the operation of distributed energy resources in electrical systems [29–31]. The description of the iterative process related to the VSA is presented in Algorithm 1.

Algorithm 1: Pseudocode vortex search algorithm.

Data: Read data electrical system and VSA and optimization parameters;
if $t = 0$ **then**
  Define μ_0 and r_0 for the vortex;
  Generate the individual of the population in a random way;
  Calculate the FF for each individual of the initial population → Matrix hourly power flow;
  Find the incumbent s^0_{best};
for $t = 1 : t_{\max}$ **do**
  Update the center $\mu_t = s^t_{best}$;
  Calculate the radius r_t;
  Generate new individuals of the potulation s^{t+1}_i;
  calculate FF for each individual s^t_i → Matrix hourly power flow;
  Find the incumbent s^t_{best};
  if $t \geq t_{\max}$ **then**
    Select μ_t as the solution to the problem;
    Return the solution and FF to the master problem;
    Break;

The VSA starts reading the data of the electrical system analyzed and the optimization parameters that were tuning by using the methodology based on the particle swarm optimization algorithm proposed in [22]. The electrical and optimization parameters are presented in Section 4.

The iterative process of the VSA starts calculating the initial center (μ_0) and radius (r_0) in the iteration zero of the algorithm ($t = 0$) or initial state. In this iteration, the VSA calculates μ_0 by using Equation (13), where x^{max} and x^{min} correspond to the maximum and minimum values of the variables associated with the problem studied—in this particular

case, the maximum and minimum power generated by the PV DGs in each hour within the horizon time.

$$\mu_0 = \frac{(x^{max} + x^{min})}{2} \tag{13}$$

To obtain r_0, we use Equation (14), where t is the current iteration, t_{max} is the maximum number of iteration of the algorithm, and a denotes a constant parameter that controls the step-down speed of the vortex radius that represents the solution space. Due to $t = 0$, in this initial state, the radius is a function of the matrix of covariances σ_0, simplified to be equal to μ_0 in this particular case, by generating that the radius of each variable be equal to the distance to the initial center.

$$r_{t+1} = \sigma_0(1 - \frac{t}{t_{max}})\epsilon^{(-a\frac{t}{t_{max}})} \tag{14}$$

After obtaining μ_0 and r_0, we generate the initial population for which we consider random values between the maximum and minimum values assigned for each variable, by verifying that all individuals satisfy the limits fix. Then, we evaluate the fitness function for each individual by using the slave stage; in this work, employing the MHPF, which evaluates the effect of the PV power injected to the DC grid by the distributed generations, by considering the power demand and conditions associated with the electrical test systems. Finally, with the FF values, we identify and select the individual with the best solution as incumbent of the problem S^0_{best}.

$$s_i^t = p(\zeta_i^t, \mu_t, v) = ((2\pi)^d|v|)^{(1/2)}e^{\left(-\frac{1}{2}\frac{(\zeta_i^t-\mu_t)^T(\zeta_i^t-\mu_t)}{v}\right)} \tag{15}$$

From the first iteration until the end of the iterative process, the VSA updates the center of the vortex ($\mu_i ter$) with the variables that comprise the incumbent in each iteration s^t_{best}. After that, the VSA calculates the r_t and generates the new population by using Equation (15). In this Equation, s_i^t corresponds to the i^th individual of the population, ζ_i^t denotes a vector of random variables, and v is a matrix of covariances. r_t is important in VSA since it limits the ζ_i^t random vector. After generating the new population, the FF of all individuals is evaluated by using the slave stage. Subsequently, the incumbent of the problem is updated in the current iteration s^t_{best}. If the number of $t_maximum$ is achieved, the optimization process finishes, selecting s^t_{best} as the variables (power dispatch of PV distributed generators) that obtain the best solution for the problem by returning the FF, generating the best economical, technical, or environmental index. In other cases, other iterations are carried out.

3.2.2. Matrix Hourly Power Flow

To evaluate the impact of the PV hourly power proposed for the different solutions provided by the master stage (VSA), we propose a matrix hourly power flow (MHPF) that uses the PV generation, power demand, and data of a test electrical system for calculating the FF. The main idea behind using this methodology is reducing the processing times associated with the operation of the slave stage, since the evaluation of FF is the stage inside the optimal operation of distributed energy resources that requires more time. We traditionally use an hourly power flow based on an iterative algorithm to calculate the effects in the objective function in each period of time, summarizing the FF function obtained for the whole operation day [22,31], as presented in Algorithm 2.

Algorithm 2: Traditional hourly power flow based on successive approximation method (SA).

Data: Data reading and assignment of HSA parameters
for $h = 1 : 24$ **do**
  Load the power demanded by the loads during period h;
  Load the active power provided by the PV DGs during period h;
  Solve the DC power flow for period h using the successive approximation method reported in [32];
  Calculate the objective function for period h
  Evaluate the constraints for period h;
  Calculate the FF for period h;
Add the FF values of all the periods;
Return the FF value to the master stage;

The traditional hourly power flow uses the power flow method based on successive approximations [32]. This method solves Equation (16) through an iterative process; by using a maximum iteration number of 2000 and a convergence error of 1×10^{-10}, these values were obtained in a heuristic way. In Equation (16), the variables of interest are the voltage profiles in the demand buses at the period h at the current iteration ($\mathbb{V}_{d,h}^{t+1}$), while the voltages in the slack buses are known, represented by $\mathbb{V}_{s,h}$. This equation is a recurrent mathematical formulation that requires the values of the demand voltage profiles in the last iteration to be solved ($\mathbb{V}_{d,h}^{t}$). The other elements that make up the equation correspond to the component of the conductance matrix associated with the slack buses, the demand buses $\mathbf{G}_{ds}$, and the component of the conductance matrix that relates the demand nodes to each other ($\mathbf{G}_{dd}$). Furthermore, $\mathbb{P}_{d,h}$ is the vector that contains the active power demanded by the loads connected to the different buses of the electrical systems at the hour h, and $\mathbb{P}_{pv,h}$ is the vector that contains the active power generated by the PV distributed generators located in the grid at the hour h. Finally, in this equation, *diag* is a diagonal matrix that allows matrix products of the Equation (16).

$$\mathbb{V}_{d,h}^{t+1} = -\mathbf{G}_{dd}\left[\mathbf{diag}(\mathbb{V}_{d,h}^{t})(\mathbb{P}_{d,h} - \mathbb{P}_{pv,h}) + \mathbf{G}_{ds}\mathbb{V}_{s,h}\right] \tag{16}$$

The proposed MHPF takes advantage of the power flow method based on SA by proposing a unique matrix equation that eliminates one of the iterative processes used for the traditional hourly power flow, by corresponding to the analysis of each period of time, reducing, in this way, the processing time required by the solution. To obtain the matrix equation of the successive approximation power flow method, this paper used the Hadamard product ($\circ$) and division ($\oslash$) that allow to take two matrices of the same dimensions and produce another matrix of the same dimension that contains the product or division of the element of the same position ij. An example of this is presented in Equations (17) and (19), respectively.

$$(\mathbf{A} \circ \mathbf{B})_{ij} = \mathbf{A}_{ij}\mathbf{B}_{ij} \tag{17}$$

$$(\mathbf{A} \oslash \mathbf{B})_{ij} = \frac{\mathbf{A}_{ij}}{\mathbf{B}_{ij}} \tag{18}$$

Equation (19) allows obtaining the MHPF. This equation uses matrices of size $|d|x|\mathcal{H}|$, where $|d|$ denotes the number of demand buses and $|\mathcal{H}|$ describes the total period analyzed inside the horizon time. The main difference, with respect to the traditional SA, is related to the possibility of obtaining a matrix of voltage demand that contains all voltages in the different period of time $\mathbb{V}_{dh}^{t+1}$, with $t+1$ being the iteration in the analysis and t being the last iteration. This is made possible by using a ones matrix (*ones*) that has Hadamard division operation with $\mathbb{V}_{dh}^{t}$, by generating a Hadamard product with the difference between the

matrix that contains the power demanded and PV generation in each bus for the different periods of time. This matrix presents a size of $|d|x|\mathcal{H}|$, too. $\mathbb{V}_{sh}$ is the matrix with the same size that contains the voltage in the slack buses for all hours, this value being constants.

$$\mathbb{V}_{dh}^{t+1} = -\mathbf{G}_{dd}^{-1}\left[(ones \oslash \mathbb{V}_{dh}^{t}) \circ (\mathbb{P}_{dh} - \mathbb{P}_{pvh}) + \mathbf{G}_{ds}\mathbb{V}_{sh}\right] \tag{19}$$

Finally, to solve the hourly power flow by using the matrix version proposed here, it is necessary to run an iterative algorithm using the same number of iteration and convergence error as SA, allowing, in this way, eliminating an iterative process with respect to the SA. As example, in this paper, we calculated the hourly power flow for the grid-connected network in a scenario without PV distributed generation by using the traditional methodology and the matrix version proposed here. The results obtained are reported in Table 1, where it can be appreciated that the MHPF achieved a reduction in processing times of 67.71% with respect to the SA. Furthermore, in this table, it is possible to appreciate that the MHPF required 178 fewer iterations than SA, converging to the same solution in terms of energy loss. With the last analysis, the authors of this work demonstrated the effectiveness of the proposed MHPF and the importance of this for solving the problem of optimal power flow of distributed energy resources in electrical grids.

Table 1. Hourly power flow numerical results.

Method	Avg. Time (ms)	Total Iterations	Energy Loss (kWh)
SA	0.7449	185	2186.2803
MHPF	0.2405	8	2186.2803

4. Test Systems, Generation and Demand Curves, and Additional Considerations

To evaluate the proposed master–slave optimization methodology for solving the problem of optimal operation of PV distributed generators in grid-connected and standalone DC networks, we considered two test feeders that are located in two different areas of operation, i.e., a grid-connected network and standalone grid, respectively. For the grid-connected network, we implemented the 33 bus test feeder, which was used to emulate the behavior of the solar resource and the power demand of the city of Medellín-Antioquia, Colombia, corresponding to the urban area that is connected to the national electrical network. In the same way, for the standalone network, we used a 27 bus test feeder, which was adapted to emulate the behavior of the power generation and demand of the municipality of Capurganá-Choco, Colombia, corresponding to the standalone network that operates with diesel.

4.1. Grid-Connected Test Feeder

This test feeder is an adaptation of the 33 bus AC radial system, originally proposed in [33], commonly used to evaluate new solution methodologies for the optimal power flow problem. This system contains 33 nodes and 32 distribution lines, as shown in Figure 3. To convert this system into a DC network only, it is necessary to eliminate the reactive components of the branches and loads, respectively. Furthermore, we used as base values a voltage of 12.66 kV and a power base of 100 kVA. Parametric information related to power consumption at the nodes and distribution line parameters are listed in Table 2, presenting, from left to right, the line number, send bus, receive bus, resistance of the branch that connects the send bus with the receive bus, the power demand by the load connected to the receive bus, and the maximum current allowed in each distribution line. The current limit values were computed using a power flow solution under peak conditions without PV distributed generation, by using, for the maximum currents, the Colombian Technical Standard (NTC) 2050, assuming that the conductors that can be assigned to these lines will operate under a nominal temperature of 60 °C.

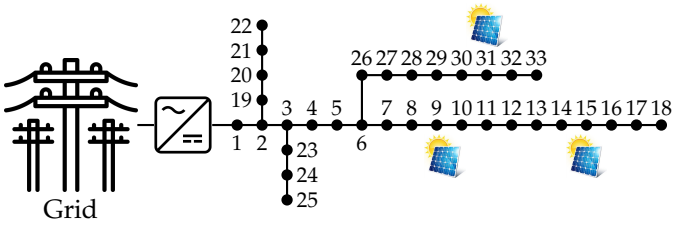

Figure 3. Electrical configuration of the grid-connected DC network.

Finally, to evaluate the effect of PV generation in the grid-connected system, three PV sources with nominal rates of 2400 kW were added to nodes 12, 15, and 31, respectively.

Table 2. Parametric information of the grid-connected network.

Line l	Node i	Node j	R_{ij} (Ω)	P_j (kW)	I_l^{max} (A)
1	1	2	0.0922	100	320
2	2	3	0.4930	90	280
3	3	4	0.3660	120	195
4	4	5	0.3811	60	195
5	5	6	0.8190	60	195
6	6	7	0.1872	200	95
7	7	8	17114	200	85
8	8	9	10300	60	70
9	9	10	10400	60	55
10	10	11	0.1966	45	55
11	11	12	0.3744	60	55
12	12	13	14.680	60	40
13	13	14	0.5416	120	40
14	14	15	0.5910	60	25
15	15	16	0.7463	60	20
16	16	17	12890	60	20
17	17	18	0.7320	90	20
18	2	19	0.1640	90	30
19	19	20	15042	90	25
20	20	21	0.4095	90	20
21	21	22	0.7089	90	20
22	3	23	0.4512	90	85
23	23	24	0.8980	420	70
24	24	25	0.8900	420	40
25	6	26	0.2030	60	85
26	26	27	0.2842	60	85
27	27	28	10590	60	70
28	28	29	0.8042	120	70
29	29	30	0.5075	200	55
30	30	31	0.9744	150	40
31	31	32	0.3105	210	25
32	32	33	0.3410	60	20

4.2. Standalone Test Feeder

For the standalone DC test feeder, we used an adaptation of the 27 bus AC radial system, originally proposed in [34]. This system contains 27 nodes and 26 electrical lines, as shown in Figure 4. To obtain the DC version of this test system, we used the same methodology indicated for the urban network, by considering the same base values. Parametric information related to power consumption at the nodes, distribution line parameters, and maximum thermal currents are listed in Table 3. Note that, for this test system, we considered three PV sources with nominal rates of 2400 kW located at nodes 5, 9, and 19, respectively.

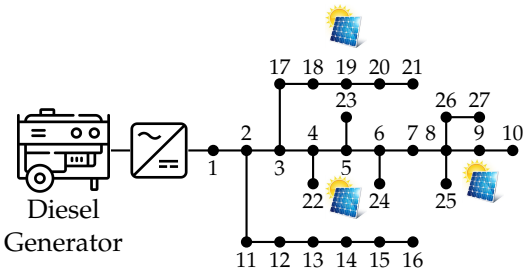

Figure 4. Electrical configuration of the standalone DC network.

Table 3. Parametric information of the standalone network.

Line l	Node i	Node j	R_{ij} (Ω)	P_j (kW)	I_l^{max} (A)
1	1	2	0.0140	0	195
2	2	3	0.7463	0	145
3	3	4	0.4052	297.5	85
4	4	5	1.1524	0	70
5	5	6	0.5261	255	70
6	6	7	0.7127	0	55
7	7	8	1.6628	212.5	55
8	8	9	5.3434	0	20
9	9	10	2.1522	266.05	20
10	2	11	0.4052	85	70
11	11	12	1.1524	340	55
12	12	13	0.5261	297.5	40
13	13	14	1.2358	191.25	25
14	14	15	2.8835	106.25	20
15	15	16	5.3434	255	20
16	3	17	1.2942	255	55
17	17	18	0.7027	127.5	40
18	18	19	3.3234	297.5	40
19	19	20	1.5172	340	20
20	20	21	0.7127	85	20
21	4	22	8.2528	106.25	20
22	5	23	9.1961	55.25	20
23	6	24	0.7463	69.7	20
24	8	25	2.0112	255	20
25	8	26	3.3234	63.75	20
26	26	27	0.5261	170	20

4.3. Test Feeders Generation Curves

The power generation based on solar resources is directly dependent on environmental conditions such as solar radiation and ambient temperature; in this sense, the output power of PV distributed generation systems can be expressed as shown in Equation (20) [35].

$$p_{i,h}^{pv} = P_i^{pv} f_{pv} \left(\frac{G_h^T}{G_i^{T,STC}} \right) \left[1 + \alpha_p \left(T_{i,h}^c - T_i^{c,STC} \right) \right], \tag{20}$$

where f_{pv} is a PV power reduction factor that considers external conditions that may affect the power production of a panel; G_h^T is the incident solar radiation on the PV distributed generator in a period of time h; $G_i^{T,STC}$ is the solar radiation of the PV distributed generator located at node i under standard test conditions; α_p is the power temperature coefficient; $T_{i,h}^c$ is the surface temperature of the PV distributed generator located at a bus i during a period of time h; and $T_i^{c,STC}$ is the surface temperature of the PV distributed generator located at a node i under standard testing conditions.

On the other hand, the surface temperature of a PV distributed generator can be calculated as shown in (21).

$$T_{i,h}^{c} = T_{h}^{a} + G_{h}^{T}\left(\frac{T_{i}^{c,NOCT} - T_{i}^{a,NOCT}}{G_{i}^{T,NOCT}}\right)\left(1 - \frac{\eta_{i}^{c}}{\alpha}\right) \quad (21)$$

where T_h^a is the ambient temperature to which the PV distributed generator is exposed in a period of time h; $T_i^{c,NOCT}$ is the nominal operating cell temperature of the PV distributed generator located at node i when exposed to radiation $G_i^{T,NOCT}$ at an ambient temperature of $T_i^{a,NOCT}$; η_i^c is the electrical efficiency of the PV distributed generator located at a node i; τ is the solar transmittance of the PV distributed generator; and α is the solar absorption of the PV distributed generator.

To determine the expected behavior of solar generation for an average day in the grid-connected and standalone networks under analysis, we considered the parametric information presented in Table 4. This information was adapted from [35,36], assuming that the PV generators were constructed with silicon polycrystalline technology.

Table 4. Parametric information related to PV distributed generators.

Parameter	Value	Unit	Parameter	Value	Unit
P_i^{pv}	100	W	f_{pv}	0.95	-
$G_i^{T,STC}$	1000	W/m^2	α_p	−0.0045	1/°C
$T_i^{c,STC}$	25	° C	$T_i^{c,NOCT}$	46	°C
$G_i^{T,NOCT}$	800	W/m^2	$T_i^{a,NOCT}$	20	° C
η_i^c	0.141	-	$\tau\alpha$	0.9	-

Setting the nominal power of the PV distributed generators at 100 W, a generation curve varying between 0 and 100 W was obtained, which can be considered as a percentage generation curve that denotes the behavior of the solar resource in the area under study (i.e., C_h^{pv}). Furthermore, to characterize the power generation based on the solar resource of the city of Medellín and the municipality of Capurganá, we used the solar radiation and the environmental temperature data provided by the National Aeronautics and Space Administration (NASA) database for each area [37]. These data were taken for the year 2019, from 1 January to 31 December, with an hourly sampling, in order to eliminate the pandemic situation related to COVID-19. The hourly average information for both areas is presented in Table 5. In addition, applying Equations (20) and (21), considering the information reported in Table 4, the average power generation for Medellín and Capurganá was obtained and is presented in Table 5 and Figure 5.

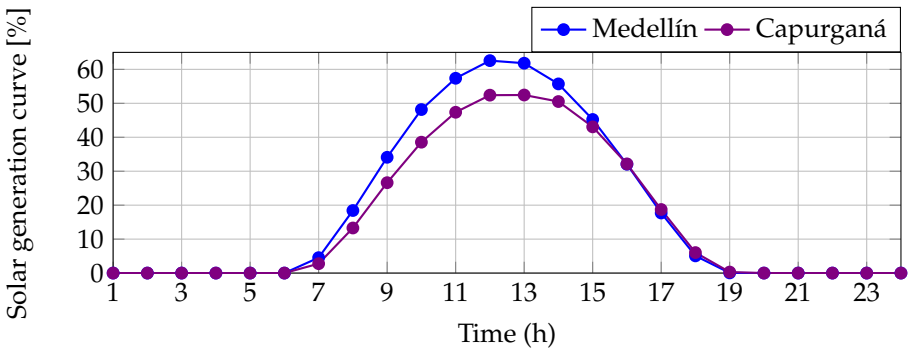

Figure 5. Expected average generation curve for Medellín and Capurganá, Colombia.

Table 5. Solar radiation data (W/m^2), ambient temperature (°C), and behavior (p.u.) for an average day in the areas under study.

Area	**Medellín (Grid-Connected)**			**Capurganá (Standalone)**		
Hour	G_T	T_a	C_{pv}	G_T	T_a	C_{pv}
1	0	16.14132	0	0	24.44252	0
2	0	15.90636	0	0	24.32474	0
3	0	15.68132	0	0	24.22545	0
4	0	15.46022	0	0	24.14674	0
5	0	15.27545	0	0	24.08422	0
6	0	15.10329	0	0	24.03482	0
7	46.02425	15.15718	0.04541	29.14570	24.10367	0.02770
8	190.83559	16.15636	0.18424	142.11066	24.78126	0.13277
9	362.83753	17.43868	0.34100	291.61926	25.68211	0.26622
10	526.64647	18.87312	0.48161	431.95384	26.63671	0.38547
11	640.99058	20.27438	0.57375	540.61581	27.47515	0.47362
12	709.05312	21.36342	0.62572	605.16362	28.10252	0.52397
13	701.86370	21.98721	0.61809	606.93027	28.46775	0.52442
14	626.82690	22.12107	0.55716	583.07479	28.56923	0.50519
15	499.86074	21.83071	0.45236	490.55904	28.42334	0.43065
16	346.26581	21.20351	0.32052	359.22033	28.03460	0.32148
17	186.66671	20.38668	0.17693	204.48775	27.44945	0.18722
18	52.33403	19.35951	0.05066	64.51775	26.69008	0.06034
19	0.50986	18.32258	0.00050	3.17460	25.89016	0.00300
20	0	17.72414	0	0	25.39227	0
21	0	17.29586	0	0	25.09285	0
22	0	16.96148	0	0	24.87663	0
23	0	16.67395	0	0	24.70841	0
24	0	16.40545	0	0	24.56926	0

4.4. Test Feeders Demand Curves

The expected average power consumption in the city of Medellín and the municipality of Capurganá was determined based on historical consumption data provided by the distribution companies operating in each area: (i) in Medellín, historical reports are made by the network operator Empresas Públicas de Medellín (EPM) [38]; (ii) in Capurganá, power consumption data were taken from IPSE reports, which is a company responsible for monitoring and supervising the noninterconnected electrical areas of Colombia in order to promote, develop, and implement energy-related solutions in these areas [39]. In both cases, the power consumption data were taken for the year 2019, from 1 January to 31 December, with an hourly sampling. In the same way as for the generation curves, in Table 6 we list the hourly average information for both areas. With the data presented in this table, the average behavior of the power demand for a typical day in Medellín and Capurganá is obtained, as shown in Figure 6.

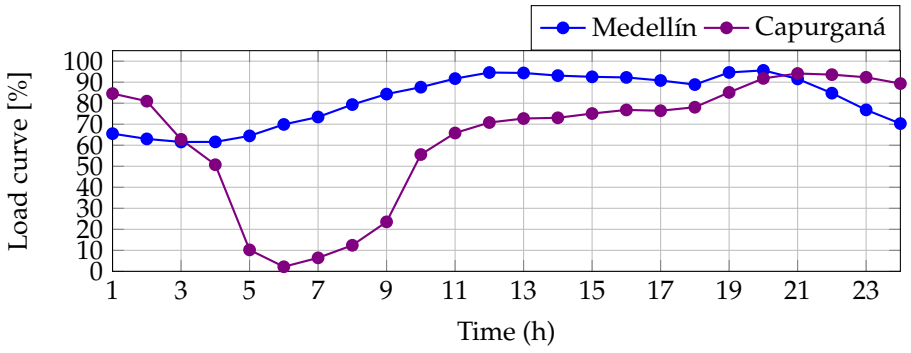

Figure 6. Expected average demand curve for Medellín and Capurganá, Colombia.

Table 6. Power consumption data (kW) and behavior (p.u.) for an average day in the areas under study.

Area	Medellín (Grid-Connected)		Capurganá (Standalone)	
Hour	P_d	$P_{d,pu}$	P_d	$P_{d,pu}$
1	1,012,876.20	0.65509	428.04117	0.84573
2	974,315.40	0.63015	409.76717	0.80962
3	951,768.01	0.61557	317.81654	0.62795
4	952,169.92	0.61583	256.70648	0.50720
5	996,601.97	0.64457	51.70864	0.10217
6	1,080,667.80	0.69894	11.05835	0.02185
7	1,135,234.91	0.73423	32.49553	0.06421
8	1,226,850.93	0.79348	62.77491	0.12403
9	1,303,895.33	0.84331	119.17381	0.23547
10	1,354,781.01	0.87622	281.26057	0.55572
11	1,417,860.03	0.91702	333.09429	0.65813
12	1,462,589.11	0.94595	358.36076	0.70805
13	1,459,381.62	0.94388	368.01140	0.72712
14	1,439,889.28	0.93127	369.70917	0.73048
15	1,430,823.70	0.92541	379.97901	0.75077
16	1,426,481.64	0.92260	388.65478	0.76791
17	1,404,019.24	0.90807	386.78365	0.76421
18	1,373,896.43	0.88859	395.19266	0.78083
19	1,463,002.74	0.94622	430.88177	0.85134
20	1,478,398.44	0.95618	464.61670	0.91800
21	1,415,579.31	0.91555	476.40313	0.94128
22	1,310,824.08	0.84779	473.67462	0.93589
23	1,187,930.28	0.76831	467.29281	0.92328
24	1,086,900.38	0.70297	452.18590	0.89344

4.5. Parametric Information for the Objective Functions Calculation

To calculate the values of the economical, technical, and environmental conditions defined in Equations (1), (3), and (4), the parametric data displayed in Table 7 were used. This table shows the purchasing energy cost by conventional generators in grid-connected and standalone grids, the costs associated with the maintenance of PV distributed generators, and the emissions factors associated with power generation in urban and rural networks.

Table 7. Parameters used to calculate the economical, technical, and environmental indexes.

Parameter	Value	Unit	Parameter	Value	Unit
$C_{kWh}^{grid-connected}$	0.1302	USD/kWh	$CE_s^{grid-connected}$	0.1644	kg/kWh
$C_{kWh}^{standalone}$	0.2913	USD/kWh	$CE_s^{standalone}$	0.2671	kg/kWh
$C_{O\&M}^{pv}$	0.0019	USD/kWh	ΔV	± 10	%

It is worth highlighting that (i) energy generation costs for the study areas were taken from reports made by networks operators to the Sistema Unico de Información (SUI) in 2019 [40,41]; (ii) the operation and maintenance costs of the PV distributed generators were taken from [42]; (iii) the emissions factor for the grid-connected network is the factor established by XM for the interconnected electrical system, to which EPM [43] belongs. Additionally, the emissions factor for the standalone grid is associated with diesel fuel consumption and was taken from the database of the Emission Factors of Colombian Fuels (FECOC) [44]; and (iv) the voltage regulation limits are set as $\pm 10\%$ of the nominal voltage of the system, as specified in the NTC 1340.

Finally, with the aim of evaluating the effectiveness and robustness of the proposed methodology, we used a total of four comparison methods reported in the literature for solving the optimal power flow problem in DC grids, by adapting these for solving the mathematical formulation described in Section 2. The first comparison method corresponds

to the crow search algorithm (CSA); this optimization method is based on hunting nature of the crows [45]. The second comparison method is the multiverse optimization algorithm (MVO) [23]; this method takes advantage of the behavior of the universe for solving problems with continuous variables. The third method corresponds to the particle swarm optimization algorithm (PSO); this method is based on the hunting behavior of birds and fish to solve continuous problems, as studied here [22]. Finally, we used the salp swarm algorithm (SSA), which is a bioinspired algorithm that uses the behavior of salps, which are fish that live in swarms and form chains as they move, which facilitates the way they move through the deep ocean in search of food [46]. All the aforementioned solution methodologies were selected as comparison methods due to the excellent results reported by the authors, allowing, in this work, the tuning of all optimization parameters with the aim of obtaining the best performance for each one. The tuning of all optimization methodologies by including the proposed VSA was carried out using methodology based on PSO reported in [31]. The optimization parameters found are reported in Table 8.

Table 8. Optimization parameters used for all solution methodologies.

Method	Optimization Parameter	Value
VSA	Number of particles	163
	Maximum iterations	762
	Nonimprovement iterations	762
	x parameter	0.08
CSA	Number of particles	177
	Maximum iterations	471
	Nonimprovement iterations	295
	Memory capacity (mc)	0.65
	Flight length (fl)	3.25
MVO	Number of particles	41
	Maximum iterations	1326
	Nonimprovement iterations	188
	Wep-min	0.68
	Wep-max	0.51
	P parameter	3
PSO	Number of particles	159
	Maximum iterations	492
	Nonimprovement iterations	229
	Maximum inertia (Wmax)	0.99
	Minimum inertia (Wmin)	0.32
	Cognitive component (C1)	0.06
	Social component (C2)	1.54
SSA	Number of particles	141
	Maximum iterations	1577
	Nonimprovement iterations	547

It is important to highlight that, in order to make a fair comparison between the continuous optimizations methods previously described, all solution methods using the MHPF are proposed here.

5. Simulation Results and Discussion

This section shows, analyzes, and discuses all results obtained by the optimization algorithms to solve the problem of optimal operation of PV distributed generators in DC networks. To accomplish this task, we employed a grid-connected and a standalone grid from Medellín and Capurganá in Colombia, respectively. To realize all the simulations, we used the numerical computing system Matlab 2022a version, by using a Dell Precision 3450 workstation with an Intel(R) Core(TM) i9-11900 CPU@2.50 GHz and 64.0 GB RAM running Windows 10 Pro 64-bit. Finally, each algorithm was executed 100 times

for each objective function, with the intention of evaluating the average solution for each index used, the standard deviation, and the average processing times required by the optimization methodologies.

The simulation section is divided into two, focusing on each test system used. Section 5.1 presents the results obtained for the standalone system, while Section 5.2 presents the grid-connected system. Each analysis evaluates the average results obtained by the algorithms, the standard deviation, and the average processing time to reach the solution for the problem studied, for the three objective functions selected in this document.

5.1. Capurganá's Network: Standalone System

Table 9 presents all simulation results obtained for the different optimization methods for each objective function used. This table is arranged from left to right as follows: the first column corresponds to the optimization algorithm employed. In the second, third, and fourth columns, we present the results related to the objective functions that we are seeking to minimize in this document (E_{loss}, E_{cost}, and E_{CO_2}), where E_{loss} is the energy losses in the grid associated with the energy transport in kW, E_{cost} is the energy purchasing cost of the conventional generators located in the DC grid in USD, and E_{CO_2} is the CO_2 emission related to the energy production in the DC grid by the conventional generators in $kgCO_2$. In the first row of this table, we present the values associated with the electrical network without PV distributed generation (base case) for each objective function. The rest of the table continues with the analysis of the average solution obtained by each solution methodology, the percentage of reduction with respect to the base case, the standard deviation obtained by each method, and the average processing time that it took each algorithm to reach the presented solution.

By analyzing the results obtained in the last table, it is possible to obtain Figure 7. This figure shows the percentage of average reduction by each method (a) with respect to base case, the percentage of standard deviation reached by each algorithm (b), and the average processing time that each algorithm needs to obtain the solution for the problem addressed, in seconds (c). In Figure 7a, we analyze the percentage of average reduction obtained by the optimization algorithms for each objective function. For the E_{loss} case, the VSA algorithm obtains an E_{loss} of 359.8317, achieving a reduction of 26.4605, outperforming SSA by 0.0045%, MVO by 0.0403%, PSO by 0.4533%, and CSA by 1.9135%. For the E_{cost} case, the proposed algorithm obtains a percentage reduction of 34.7833%, reaching an E_{cost} value of 12,055.3410, outperforming the other methodologies by an average percentage of 2.8246%. In the E_{CO_2} case, the VSA once again obtains the best solution, reaching an E_{CO_2} value of $11,016.6177\ kgCO_2$, and reaching an emissions average percentage reduction of 35.0102% in relation to the base case, outperforming SSA, MVO, PSO, and CSA by 0.1354%, 0.6781%, 1.4805%, and 8.9539%, respectively. The discussion presented shows that the VSA obtains the best average solutions for the three objective functions addressed in this document.

Figure 7b compares the solutions obtained by each optimization algorithm in terms of standard deviation in the E_{loss}, E_{cost}, and E_{CO_2} objective functions. In the first one, the VSA algorithm obtains a percentage of standard deviation of 0.0212%, beating SSA by 0.0018%, MVO by 0.2144%, PSO by 0.3883%, and CSA by 1.7335%. In the second case, related to the E_{cost}, the VSA occupies the first position, with a minor standard deviation percentage (0.3042%), outperforming SSA, PSO, CSA, and MVO by 0.1322%, 1.4669%, 2.0036%, and 2.1259%, respectively. In the third case, associated with reduction of E_{CO_2}, the proposed algorithm reaches a standard deviation value of 0.2886%, outperforming the other algorithms by an average percentage of 1.2641%. Thus, through the results obtained from Figure 7b, it is possible to observe the excellent accuracy of the VSA in terms of repeatability for standalone grids; it outperforms the other optimization algorithms in each of the objective functions used in this document, and reaches excellent-quality solutions every time the algorithm is executed.

Table 9. Simulation results obtained by the optimization algorithms in standalone system.

CAPURGANÁ'S STANDALONE SYSTEM			
Objective function	$E_{loss}(kWh)$	$E_{cost}(USD)$	E_{CO_2} $(kgCO_2)$
Base case	**489.3042**	**18,485.0507**	**16,951.2974**
Average solution			
Algorithm	E_{loss}	E_{cost}	E_{CO_2}
VSA	359.8317	12,055.3410	11,016.6177
CSA	369.1944	13,663.8328	12,534.4183
MVO	360.0291	12,231.1691	11,131.5617
PSO	362.0496	12,340.2908	11,267.5734
SSA	359.8537	12,074.5543	11,039.5781
Percentage of average reduction (%)			
Algorithm	E_{loss}	E_{cost}	E_{CO_2}
VSA	26.4605	34.7833	35.0102
CSA	24.5471	26.0817	26.0563
MVO	26.4202	33.8321	34.3321
PSO	26.0073	33.2418	33.5297
SSA	26.4560	34.6794	34.8747
STD (%)			
Algorithm	E_{loss}	E_{cost}	E_{CO_2}
VSA	0.0212	0.3042	0.2886
CSA	1.7548	2.3077	2.1093
MVO	0.2356	2.4301	2.0192
PSO	0.4095	1.7711	1.6491
SSA	0.0230	0.4363	0.4329
Time (s)			
Algorithm	E_{loss}	E_{cost}	E_{CO_2}
VSA	7.69	7.84	7.78
CSA	6.54	6.76	6.74
MVO	2.02	1.80	1.90
PSO	4.21	4.43	4.44
SSA	12.59	12.90	13.12

Figure 7c compares the average time employed by each method to obtain the solution for each objective function used. In the E_{loss} case, the VSA algorithm obtains an average processing time of 7.69 s, being surpassed by the MVO, PSO, and CSA algorithms, which obtain 2.02 s, 4.21 s, and 6.54 s, respectively, with the proposed methodology being faster than the SSA algorithm, which requires an average time of 12.59 s. In the E_{cost} case, the proposed algorithm reaches an average processing time of 7.84 s, requiring more time than the MVO, PSO, and CSA algorithms, which obtain 1.8 s, 4.43 s, and 6.76 s, but surprisingly less time than the SSA algorithm, which reaches a 12.9 s average time value. In the E_{CO_2} case, the VSA algorithm obtains an average processing time of 7.78 s, beating the MVO, PSO, and CSA algorithms by 6.05 s, 3.41 s, and 1.08 s; reducing the processing time required by the SSA algorithm by 5.06 s. Although the VSA algorithm does not have the shortest processing time, it is important to note that the proposed algorithm takes only 7.77 seconds on average to reach the best average solution to solve the problem addressed in the E_{loss}, E_{cost}, and E_{CO_2} objective functions for a whole operation day, which is a reduced time in terms of grid operation. However, to demonstrate that the VSA algorithm is the method with the best trade-off between solution quality and processing time for solving the problem of optimal operation of PV distributed generators in standalone DC networks, Table 10 is presented.

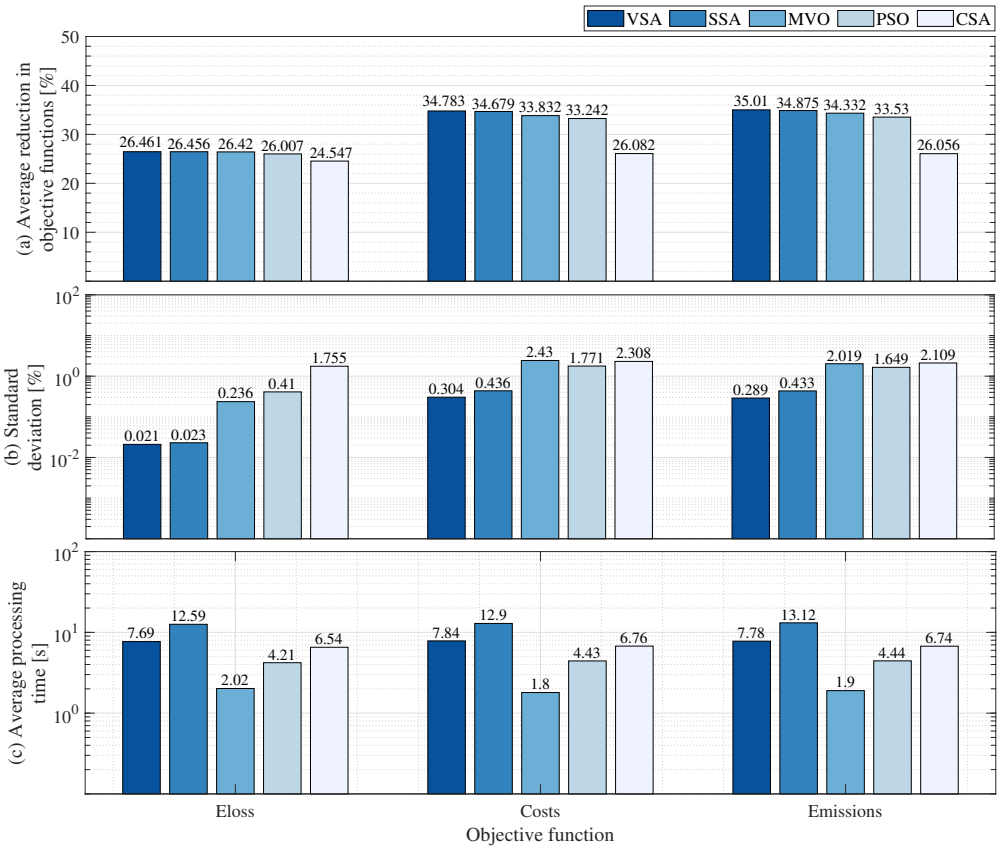

Figure 7. Average reductions, standard deviation, and average processing time obtained by optimization methods in economical, technical, and environmental conditions used in standalone network.

The previous table is arranged from left to right as follows: the optimization algorithm and the objective function results, ordering the results with the aim to present the average solution obtained and processing time; presenting, at the end, the distance with respect to the origin ($(0,0)$ point) which graphically represents the best solution to the problem in Figure 8. It represents 0 E_{loss} (Figure 8a), 0 E_{cost} (Figure 8b), and 0 E_{CO_2} (Figure 8c) with a 0 s processing time requirement, with respect to all scenarios generated by the different objective functions used. In Figure 8, we fix the x-axis to the objective function analyzed, and on the y-axis is the average processing time required by each solution methodology. It is important to mention that to calculate the distance from the origin to the optimization algorithms, the Pythagorean theorem was used, by considering the objective function and the average processing time data.

Table 10 and Figure 8 demonstrate that the VSA optimization algorithm is the technique that obtains the best trade-off between average solution and processing time for the different objective functions used. In all scenarios, the VSA achieved the minor distance with respect to the origin, which means that the VSA obtained the minor objective function value and processing time. This shows that the proposed methodology has an excellent impact on the solution quality for the problem of optimal operation of PV distributed generators in standalone DC networks in each of the objective functions, by presenting reduced processing time. Therefore, the VSA algorithm is the technique that allows to obtain the best results when technical, economical, and environmental indexes are analyzed and the processing time required is considered for an isolated network.

Table 10. Average objective function solution vs. average processing time in standalone system.

Energy Losses (Figure 8a)			
Method	E_{loss} (kWh)	**Time (s)**	**Distance to the origin**
VSA	359.8317	7.69	359.9139
CSA	369.1944	6.54	369.2522
MVO	360.0291	2.02	360.0348
PSO	362.0496	4.21	362.0741
SSA	359.8537	12.59	360.0739
Costs (Figure 8b)			
Method	E_{cost} (USD)	**Time (s)**	**Distance to the origin**
VSA	12,055.3410	7.84	12,055.3436
CSA	13,663.8328	6.76	13,663.8345
MVO	12,231.1691	1.80	12,231.1693
PSO	12,340.2908	4.43	12,340.2916
SSA	12,074.5543	12.90	12,074.5612
Emissions (Figure 8c)			
Method	E_{CO_2} $(kgCO_2)$	**Time (s)**	**Distance to the origin**
VSA	11,016.6177	7.78	11,016.6205
CSA	12,534.4183	6.74	12,534.4201
MVO	11,131.5617	1.90	11,131.5619
PSO	11,267.5734	4.44	11,267.5743
SSA	11,039.5781	13.12	11,039.5858

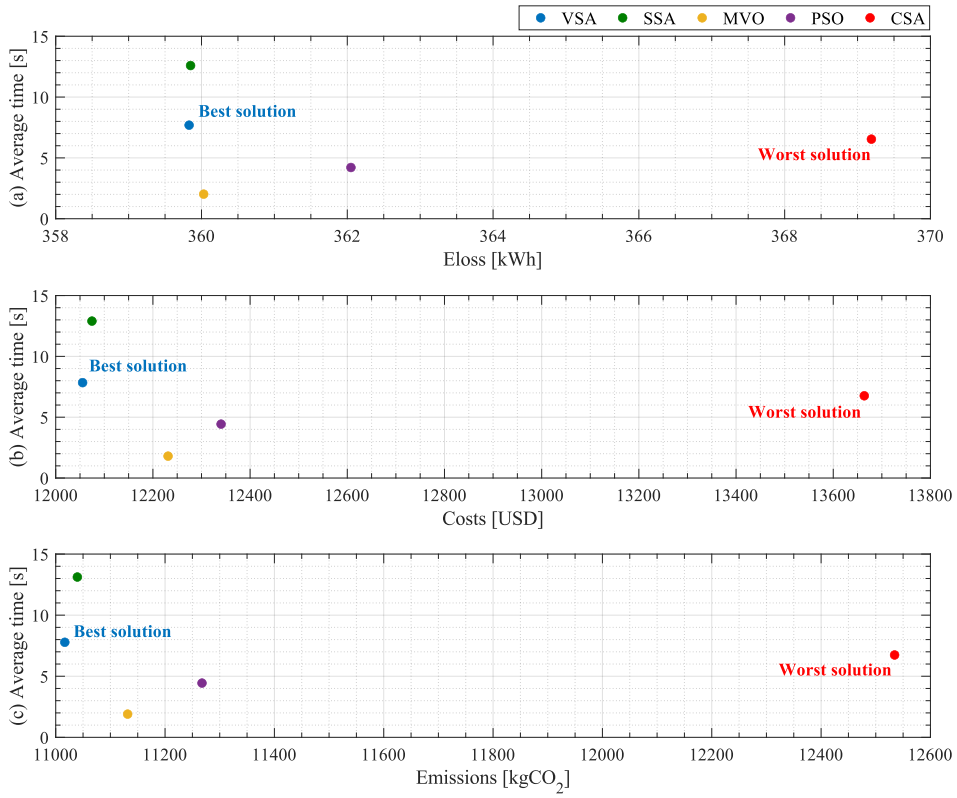

Figure 8. Trade-off provided by the optimization algorithms between objective function and required processing time in the standalone system.

5.2. Medellín's Network: Grid-Connected System

In this subsection, we analyze the results obtained by all optimization algorithms in the grid-connected system studied. To achieve this, Table 11 is arranged in the same form as Table 9. In the first row of this table, we present values obtained in the test system without considering the inject of PV power by the DGs in relation to the E_{loss}, E_{cost}, and E_{CO_2}, respectively. The analysis continues, showing the results obtained by each algorithm in terms of average solution, percentage of average reduction obtained by each solution methodology with respect to the base case, the standard deviation obtained by each method, and, finally, analyzing the average processing time required by each optimization algorithm after 1000 executions.

Table 11. Simulation results obtained by the optimization algorithms in grid-connected system.

MEDELLÍN'S GRID-CONNECTED SYSTEM			
Objective function	$E_{loss}(kWh)$	$E_{cost}(USD)$	E_{CO_2} $(kgCO_2)$
Base case	**2186.2803**	**9776.3892**	**12,345.1497**
Average solution			
Algorithm	E_{loss}	E_{cost}	E_{CO_2}
VSA	1225.2909	7249.3825	9108.9096
CSA	1270.1562	7407.9046	9328.7685
MVO	1231.2531	7298.7157	9187.9682
PSO	1268.5973	7392.0432	9282.4081
SSA	1225.3323	7297.9712	9166.6746
Percentage of average reduction (%)			
Algorithm	E_{loss}	E_{cost}	E_{CO_2}
VSA	43.9555	25.8481	26.2147
CSA	41.9033	24.2266	24.4337
MVO	43.6827	25.3434	25.5743
PSO	41.9746	24.3888	24.8093
SSA	43.9536	25.3511	25.7468
STD (%)			
Algorithm	E_{loss}	E_{cost}	E_{CO_2}
VSA	0.0108	0.5697	0.5676
CSA	1.3806	1.8500	1.6987
MVO	2.2694	1.2190	1.5868
PSO	2.4065	2.2579	2.0891
SSA	0.0131	0.7089	0.6306
Time (s)			
Algorithm	E_{loss}	E_{cost}	E_{CO_2}
VSA	9.93	10.37	10.45
CSA	36.37	36.45	36.87
MVO	2.45	2.47	2.48
PSO	5.96	6.47	6.60
SSA	20.85	21.47	21.29

By analyzing the results described in this table, it is possible to obtain Figure 9, where the results achieved by each algorithm are shown. This figure illustrates the percentage of reduction with respect to base case (Figure 9a), the percentage of standard deviation obtained by each algorithm (Figure 9b), and the average processing time required to reach the average solution (Figure 9c) in relation to the objective functions used.

In relation to the reductions obtained with respect to the base case, in the particular case of energy losses, Figure 9a shows that the VSA algorithm reaches a reduction in average E_{loss} of 43.9555%, outperforming the SSA by 0.0019%, MVO by 0.2727%, PSO by 1.9808%, and the CSA by 2.0521%. In the costs stage, the proposed algorithm obtains an

E_{cost} value of 7249.3825, reducing 25.8481% with respect to base case, outperforming the SSA, MVO, PSO, and CSA algorithms by 0.4970, 0.5046, 1.4592, and 1.6215, respectively. In the case of emissions, the VSA method obtains an E_{CO_2} value of 12,345.1497, ranking as the algorithm that achieves the best reduction with a percentage of 26.2147%, outperforming the other techniques by an average percentage of 1.0737%. The last discussion demonstrates that the VSA algorithm allows obtaining the best average reduction for solving the optimal operation problem of distributed photovoltaic generators in DC grids, allowing the grid operator to perform the most optimal grid planning for a day of operation in technical, economical, and environmental terms for grid-connected networks.

To evaluate the accuracy presented by each algorithm, Figure 9b is presented. This figure compares the standard deviation obtained by each method to solve the problem of optimal operation of PV distributed generators in grid-connected DC networks in the three objective functions. In the energy losses case, the VSA algorithm obtains the best percentage of standard deviation with a value of 0.0108%, outperforming the other algorithms by an average percentage of 1.5067%. By analyzing the objective function related to the energy costs, the VSA ranks first, with a standard deviation percentage of 0.5697%, beating SSA by 0.1393%, MVO by 0.6493%, CSA by 1.2804%, and PSO by 1.6883%. In the emissions case, once again, the VSA obtains the best percentage of standard deviation with a value of 0.5676%, ranking as the best solution methodology with an average reduction of 0.9337%. These results show excellence in terms of solution quality and repeatability of the proposed algorithm in grid-connected networks.

Finally, with the intention of analyzing the processing time required by the solutions, Figure 9c is presented. This figure compares the average processing time required by each optimization algorithm. In the E_{loss} terms, the VSA is positioned third, with an average processing time of 9.93 s, behind the MVO and the PSO, which obtain times of 2.45 s and 5.96 s, respectively, and reducing the times reported by SSA and CSA, which are positioned fourth and fifth, with average processing times of 20.85 s and 36.37 s. In the E_{cost} case, the VSA algorithm is outperformed by MVO and PSO just by 7.9 s and 3.9 s, respectively, but the VSA reduces the processing time reported by the SSA by 11.09 s and the CSA by 26.07 s. In the analysis of E_{CO_2}, the VSA ranked third behind the MVO and PSO just by 7.97 s and 3.85 s, but outperformed SSA and CSA by 10.85 s and 26.42 s. The average processing times discussed above show that the fastest optimization algorithms are MVO and PSO; however, these algorithms become stuck in local optima because not enough processing time is used in the exploration phase. On the other hand, the VSA has more adequate exploration and exploitation phases in comparison with the other optimization algorithms, allowing it to escape from local optima and find solutions of high quality in lower processing times, for each objective function employed.

Finally, for a standalone network, with the aim to identify the optimization algorithm with the best trade-off between solution quality and processing time, Table 12 is presented. This table is arranged in the same order as Table 10. Through this table, is possible to obtain Figure 10, where the average solution of each objective function vs. average processing time are plotted, by again considering the solution with the minor distance to the origin as the best solution methodology.

The results plotted in Figure 10 demonstrate that the VSA had the capacity to solve the problem of optimal operation of PV DGs in grid-connected in DC networks with the best trade-off between technical, economical, and environmental stages, and processing times. These results allow the network operator to perform operation of a grid-connected system in shorter processing times, achieving large reductions in energy losses, operating costs, and power purchases from the grid, and also greatly reducing greenhouse gas emissions to the environment.

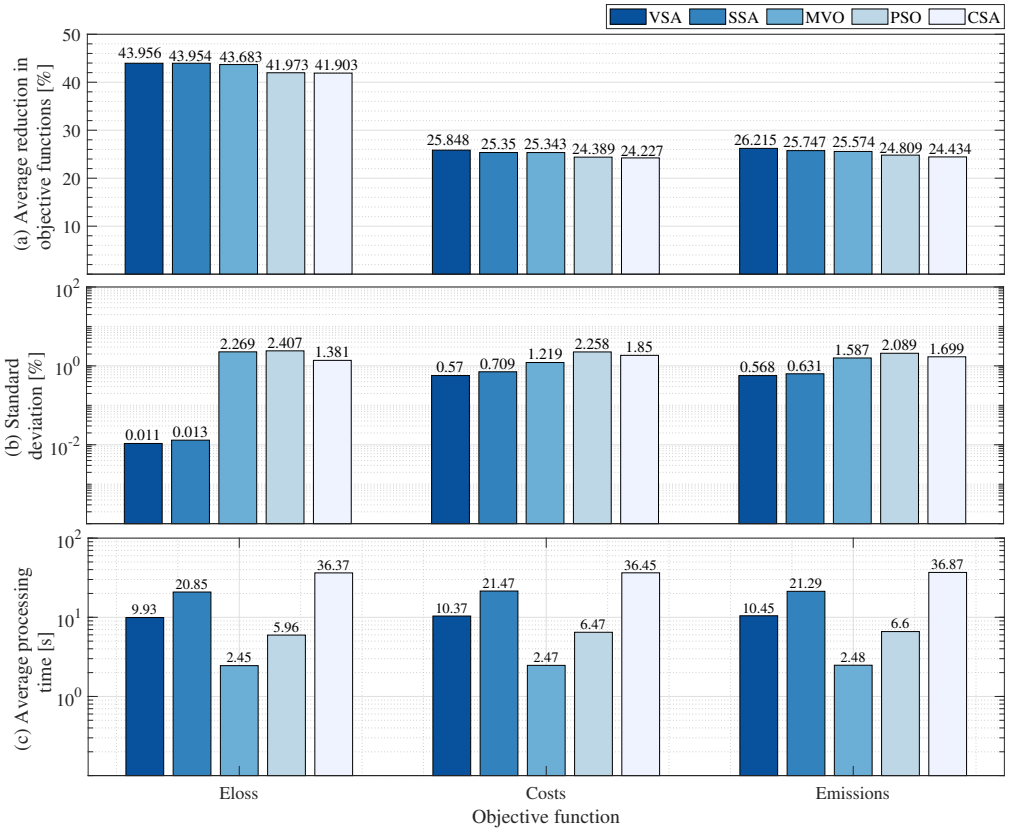

Figure 9. Average reductions, standard deviation, and average processing time obtained by optimization methods in economical, technical, and environmental conditions used in standalone network.

Table 12. Average objective function solution vs. average processing time in standalone system.

Energy Losses (Figure 10a)			
Method	$E_{loss}(kWh)$	**Time(s)**	**Distance to the origin**
VSA	1225.2909	9.93	1225.3312
CSA	1270.1562	36.37	1270.6767
MVO	1231.2531	2.45	1231.2555
PSO	1268.5973	5.96	1268.6113
SSA	1225.3323	20.85	1225.5097
Costs (Figure 10b)			
Method	$E_{cost}(USD)$	**Time(s)**	**Distance to the origin**
VSA	7249.3825	10.37	7249.3899
CSA	7407.9046	36.45	7407.9943
MVO	7298.7157	2.47	7298.7161
PSO	7392.0432	6.47	7392.0461
SSA	7297.9712	21.47	7298.0028
Emissions (Figure 10c)			
Method	$E_{CO_2}(kgCO_2)$	**Time(s)**	**Distance to the origin**
VSA	9108.9096	10.45	9108.9155
CSA	9328.7685	36.87	9328.8414
MVO	9187.9682	2.48	9187.9685
PSO	9282.4081	6.60	9282.4104
SSA	9166.6746	21.29	9166.6993

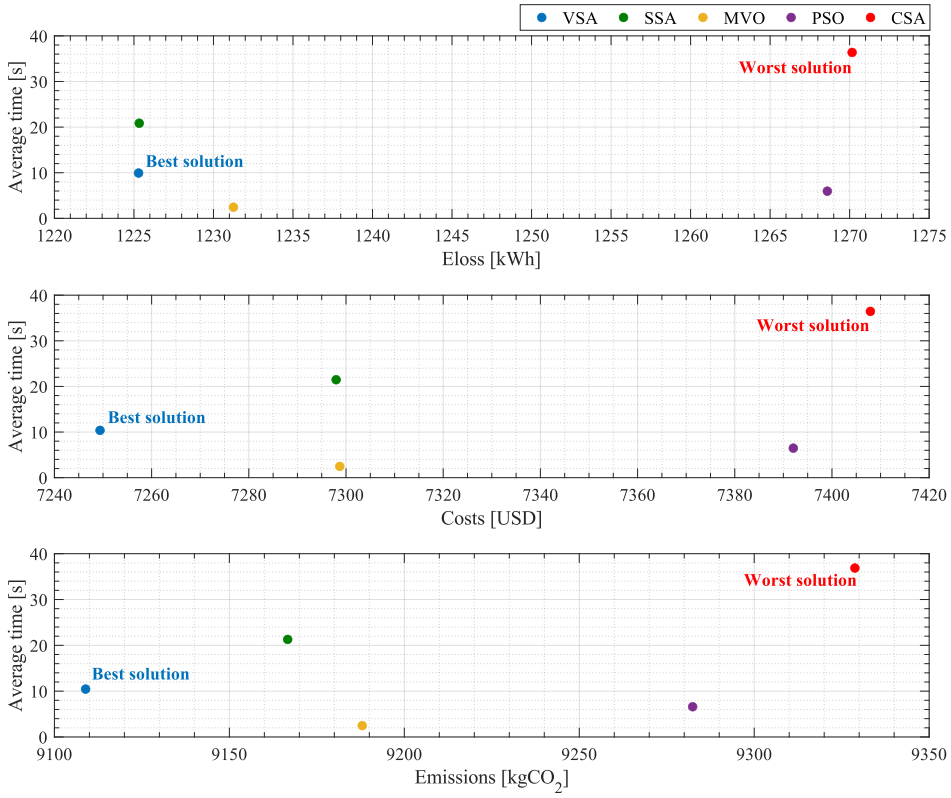

Figure 10. Trade-off provided by the optimization algorithms between objective function and required processing time in the grid-connected system.

6. Conclusions and Future Work

This document proposes a master–slave methodology to solve the problem of optimal operation of photovoltaic distributed generators in standalone and grid-connected systems in DC networks. In the master stage we employed the Vortex Search algorithm, which was used to find the power dispatch of the distributed generator located on the grid, while the slave stage used a matrix hourly power flow for calculating the effect of the power values provided by each solution generated by the master stage by considering technical, economical, and environmental objective functions, evaluating all constraints that represent the problem. Using a fitness function allowed the optimization algorithm to explore nonfeasible regions by improving the exploration and reducing the processing times. To evaluate the effectiveness of the solution methodology proposed, two test systems were used: a standalone DC system that considered the solar irradiation and power demand of Capurganá-Choco for one day of operation; and a grid-connected DC grid that used the same data reported for Medellín-Antioquia. In both systems, we used the local data for obtaining the energy losses, operational costs of the grid, and CO_2 emissions generated by the conventional generators. As comparison methods, we employed four optimization methodologies: a particle swarm algorithm, the salps swarm algorithm, the multiverse optimizer, and the crow swarm algorithm. All of them were tuned using the PSO algorithm, with the aim of obtaining the best performance to solve the problem studied.

The results obtained in this document demonstrate that the proposed master–slave methodology VSA/MHPF obtained the best solution with the minor standard deviation in both test systems for all objective functions used. In numerical terms, the VSA algorithm obtained an average reduction by considering all objective functions of 32.08% with respect to base case in the standalone Capurganá's system, and in the Medellín's grid-connected system, it achieved an average reduction of 32.01% with respect to base case in general terms, too, by improving the results obtained for all comparison methods used. These results demonstrate that the VSA algorithm has the capacity to obtain the best average solution

in E_{loss}, E_{cost}, and E_{CO_2} objective functions in relation to the other optimization methods used. In relation to the standard deviation values, the VSA presented an average standard deviation percentage of 0.2047% in the standalone system and 0.3827% in the grid-connected network; these values were the lowest obtained in all analyses carried out. These standard deviation percentages guarantee that every time the proposed methodology is executed, the solution will be near to the best average solution reported. In terms of processing time, the VSA required an average processing time of 7.77 seconds in the standalone network, while for the grid-connected network, the VSA spent an average processing time of 10.25 seconds; this is a shorter processing time when considering the planning of a whole operation day. Finally, it is possible to appreciate that all solution methodologies obtained reduced processing times, which is directly related to the implementation of the proposed matrix hourly power flow which guarantees the convergence of the solutions in shorter processing times.

The proposed methodology was not the faster method; however, the methods that obtained the best results for processing times were trapped in local optima. For this reason, in this paper it was necessary to demonstrate, in Section 5, through Figures 8 and 10, that the VSA is the algorithm that presented the best trade-off between quality solution and processing times in grid-connected and standalone DC networks.

For future work, the adaptation of the VSA as a multiobjective optimization algorithm could be considered, by considering all objective functions and others, such as chargeability, voltage stability, etc. Furthermore, the implementation of wind generators, batteries, and energy storage elements could be considered, with the intention of enhancing the economical resources of isolated and DC grid-connected grids.

Author Contributions: Conceptualization, methodology, software, and writing (review and editing), L.F.G.-N., A.A.R.-M., B.C.-C., O.D.M. and F.A. All authors have read and agreed to the published version of the manuscript.

Funding: This material is based upon work supported by the U.S. Department of Energy's Office of Energy Efficiency and Renewable Energy (EERE) under the Solar Energy Technologies Office Award Number DE-EE0002243-2144. In colaboration with the Universidad de Talca, Intituto Tecnológico Metropolinato y Universidad Distrital Francisco José de Caldas.

Institutional Review Board Statement: Not applicable.

Informed Consent Statement: Not applicable.

Data Availability Statement: No new data were created or analyzed in this study. Data sharing is not applicable to this article.

Acknowledgments: This work was developed through the collaborative work between the Universidad de Talca-Chile, Instituto Tecnológico Metropolitano de Medellín-Colombia, Universidad Distrital Francisco José de Caldas, and the University of Puerto Rico.

Conflicts of Interest: The authors declare no conflict of interest.

References

1. Saeed, M.H.; Fangzong, W.; Kalwar, B.A.; Iqbal, S. A Review on Microgrids' Challenges & Perspectives. *IEEE Access* **2021**, *9*, 166502–166517.
2. Löfquist, L. Is there a universal human right to electricity? *Int. J. Hum. Rights* **2020**, *24*, 711–723. [CrossRef]
3. Sarkodie, S.A.; Adams, S. Electricity access, human development index, governance and income inequality in Sub-Saharan Africa. *Energy Rep.* **2020**, *6*, 455–466. [CrossRef]
4. Saint Akadiri, S.; Alola, A.A.; Olasehinde-Williams, G.; Etokakpan, M.U. The role of electricity consumption, globalization and economic growth in carbon dioxide emissions and its implications for environmental sustainability targets. *Sci. Total. Environ.* **2020**, *708*, 134653. [CrossRef] [PubMed]
5. Lamb, W.F.; Wiedmann, T.; Pongratz, J.; Andrew, R.; Crippa, M.; Olivier, J.G.J.; Wiedenhofer, D.; Mattioli, G.; Khourdajie, A.A.; House, J.; et al. A review of trends and drivers of greenhouse gas emissions by sector from 1990 to 2018. *Environ. Res. Lett.* **2021**, *16*, 073005. [CrossRef]
6. Valencia, A.; Hincapie, R.A.; Gallego, R.A. Optimal location, selection, and operation of battery energy storage systems and renewable distributed generation in medium–low voltage distribution networks. *J. Energy Storage* **2021**, *34*, 102158. [CrossRef]

7. Abdelgawad, H.; Sood, V.K. A comprehensive review on microgrid architectures for distributed generation. In Proceedings of the 2019 IEEE Electrical Power and Energy Conference (EPEC), IEEE, Montreal, QC, Canada, 6–18 October 2019; pp. 1–8.
8. Li, J.; Liu, F.; Wang, Z.; Low, S.H.; Mei, S. Optimal power flow in stand-alone DC microgrids. *IEEE Trans. Power Syst.* **2018**, *33*, 5496–5506. [CrossRef]
9. Garcés, A. On the convergence of Newton's method in power flow studies for DC microgrids. *IEEE Trans. Power Syst.* **2018**, *33*, 5770–5777. [CrossRef]
10. Tawalbeh, M.; Al-Othman, A.; Kafiah, F.; Abdelsalam, E.; Almomani, F.; Alkasrawi, M. Environmental impacts of solar photovoltaic systems: A critical review of recent progress and future outlook. *Sci. Total. Environ.* **2021**, *759*, 143528. [CrossRef]
11. Moreno, C.; Milanes, C.B.; Arguello, W.; Fontalvo, A.; Alvarez, R.N. Challenges and perspectives of the use of photovoltaic solar energy in Colombia. *Int. J. Electr. Comput. Eng.* **2022**, *12*, 4521–4528. [CrossRef]
12. López, A.R.; Krumm, A.; Schattenhofer, L.; Burandt, T.; Montoya, F.C.; Oberländer, N.; Oei, P.Y. Solar PV generation in Colombia-A qualitative and quantitative approach to analyze the potential of solar energy market. *Renew. Energy* **2020**, *148*, 1266–1279. [CrossRef]
13. Insuasty-Reina, J.G. A system dynamics model for the analysis of CO2 emissions derived from the inclusion of hydrogen obtained from coal in the energy matrix in Colombia. *Int. J. Energy Econ. Policy* **2022**, *12*, 72–82. [CrossRef]
14. Li, C.; De Bosio, F.; Chen, F.; Chaudhary, S.K.; Vasquez, J.C.; Guerrero, J.M. Economic dispatch for operating cost minimization under real-time pricing in droop-controlled DC microgrid. *IEEE J. Emerg. Sel. Top. Power Electron.* **2016**, *5*, 587–595. [CrossRef]
15. Gao, S.; Jia, H.; Marnay, C. Techno-economic evaluation of mixed AC and DC power distribution network for integrating large-scale photovoltaic power generation. *IEEE Access* **2019**, *7*, 105019–105029. [CrossRef]
16. Tan, Q.; Ding, Y.; Ye, Q.; Mei, S.; Zhang, Y.; Wei, Y. Optimization and evaluation of a dispatch model for an integrated wind-photovoltaic-thermal power system based on dynamic carbon emissions trading. *Appl. Energy* **2019**, *253*, 113598. [CrossRef]
17. Younes, Z.; Alhamrouni, I.; Mekhilef, S.; Reyasudin, M. A memory-based gravitational search algorithm for solving economic dispatch problem in micro-grid. *Ain Shams Eng. J.* **2021**, *12*, 1985–1994. [CrossRef]
18. Velasquez, O.S.; Montoya Giraldo, O.D.; Garrido Arevalo, V.M.; Grisales Norena, L.F. Optimal power flow in direct-current power grids via black hole optimization. *Adv. Electr. Electron. Eng.* **2019**, *17*, 24–32. [CrossRef]
19. Garzon-Rivera, O.; Ocampo, J.; Grisales-Noreña, L.; Montoya, O.; Rojas-Montano, J. Optimal power flow in Direct Current Networks using the antlion optimizer. *Stat. Optim. Inf. Comput.* **2020**, *8*, 846–857. [CrossRef]
20. Radosavljević, J.; Arsić, N.; Milovanović, M.; Ktena, A. Optimal placement and sizing of renewable distributed generation using hybrid metaheuristic algorithm. *J. Mod. Power Syst. Clean Energy* **2020**, *8*, 499–510. [CrossRef]
21. Montoya, O.D.; Grisales-Noreña, L.F.; Gil-González, W.; Alcalá, G.; Hernandez-Escobedo, Q. Optimal location and sizing of PV sources in DC networks for minimizing greenhouse emissions in diesel generators. *Symmetry* **2020**, *12*, 322. [CrossRef]
22. Grisales-Noreña, L.F.; Montoya, O.D.; Ramos-Paja, C.A. An energy management system for optimal operation of BSS in DC distributed generation environments based on a parallel PSO algorithm. *J. Energy Storage* **2020**, *29*, 101488. [CrossRef]
23. Rosales-Muñoz, A.A.; Grisales-Noreña, L.F.; Montano, J.; Montoya, O.D.; Perea-Moreno, A.J. Application of the multiverse optimization method to solve the optimal power flow problem in direct current electrical networks. *Sustainability* **2021**, *13*, 8703. [CrossRef]
24. Sahoo, R.R.; Ray, M. PSO based test case generation for critical path using improved combined fitness function. *J. King Saud-Univ.-Comput. Inf. Sci.* **2020**, *32*, 479–490. [CrossRef]
25. Zhang, X.; Beram, S.M.; Haq, M.A.; Wawale, S.G.; Buttar, A.M. Research on algorithms for control design of human–machine interface system using ML. *Int. J. Syst. Assur. Eng. Manag.* **2021**, *13*, 462–469. [CrossRef]
26. Jin, Y.; Olhofer, M.; Sendhoff, B. A framework for evolutionary optimization with approximate fitness functions. *IEEE Trans. Evol. Comput.* **2002**, *6*, 481–494.
27. Grisales-Noreña, L.F.; Montoya, O.D.; Hernández, J.C.; Ramos-Paja, C.A.; Perea-Moreno, A.J. A Discrete-Continuous PSO for the Optimal Integration of D-STATCOMs into Electrical Distribution Systems by Considering Annual Power Loss and Investment Costs. *Mathematics* **2022**, *10*, 2453. [CrossRef]
28. Özkış, A.; Babalık, A. A novel metaheuristic for multi-objective optimization problems: The multi-objective vortex search algorithm. *Inf. Sci.* **2017**, *402*, 124–148. [CrossRef]
29. Fathy, A.; Abd Elaziz, M.; Alharbi, A.G. A novel approach based on hybrid vortex search algorithm and differential evolution for identifying the optimal parameters of PEM fuel cell. *Renew. Energy* **2020**, *146*, 1833–1845. [CrossRef]
30. Altintasi, C.; Aydin, O.; Taplamacioglu, M.C.; Salor, O. Power system harmonic and interharmonic estimation using Vortex Search Algorithm. *Electr. Power Syst. Res.* **2020**, *182*, 106187. [CrossRef]
31. Grisales-Noreña, L.; Montoya-Giraldo, O.; Gil-González, W. Optimal Integration of Distributed Generators into DC Microgrids Using a Hybrid Methodology: Genetic and Vortex Search Algorithms. *Arab. J. Sci. Eng.* **2022**, *47*, 14657–14672. [CrossRef]
32. Montoya, O.D.; Garrido, V.M.; Gil-González, W.; Grisales-Noreña, L.F. Power flow analysis in DC grids: Two alternative numerical methods. *IEEE Trans. Circuits Syst. Ii: Express Briefs* **2019**, *66*, 1865–1869. [CrossRef]
33. Baran, M.E.; Wu, F.F. Network reconfiguration in distribution systems for loss reduction and load balancing. *IEEE Power Eng. Rev.* **1989**, *9*, 101–102. [CrossRef]

34. Falaghi, H.; Ramezani, M.; Haghifam, M.R.; Milani, K.R. Optimal selection of conductors in radial distribution systems with time varying load. In Proceedings of the CIRED 2005-18th International Conference and Exhibition on Electricity Distribution, IET, Turin, Italy, 6–9 June 2005; pp. 1–4.
35. Hassan, Q.; Jaszczur, M.; Przenzak, E.; Abdulateef, J. The PV cell temperature effect on the energy production and module efficiency. *Contemp. Probl. Power Eng. Environ. Prot.* **2016**, *33*, 1.
36. Schwingshackl, C.; Petitta, M.; Wagner, J.; Belluardo, G.; Moser, D.; Castelli, M.; Zebisch, M.; Tetzlaff, A. Wind Effect on PV Module Temperature: Analysis of Different Techniques for an Accurate Estimation. *Energy Procedia* **2013**, *40*, 77–86. [CrossRef]
37. NASA. NASA Prediction Of Worldwide Energy Resources, Washington D. C., United States. Available online: https://power.larc.nasa.gov/ (accessed on 21 September 2022).
38. XM SA ESP. Sinergox Database, Colombia. Available online: https://sinergox.xm.com.co/Paginas/Home.aspx (accessed on 21 September 2022).
39. Instituto de Planificación y Promoción de Soluciones Energéticas para Zonas No Interconectadas. Informes Mensuales de Telimetría, Colombia. Available online: https://ipse.gov.co/cnm/informe-mensuales-telemetria/ (accessed on 21 September 2022).
40. Sistema Único de Información de Servicios Públicos Domicialiarios. Consolidado de Energía por Empresa y Departamento, Colombia. Available online: https://sui.superservicios.gov.co/Reportes-del-sector/Energia/Reportes-comerciales/Consolidado-de-energia-por-empresa-y-departamento (accessed on 21 September 2022).
41. Sistema Único de Información de Servicios Públicos Domicialiarios. Consolidado de Información téCnica Operativa ZNI, Colombia. Available online: https://sui.superservicios.gov.co/Reportes-del-sector/Energia/Reportes-comerciales/Consolidado-de-informacion-tecnica-operativa-ZNI (accessed on 21 September 2022).
42. Wang, P.; Wang, W.; Xu, D. Optimal sizing of distributed generations in DC microgrids with comprehensive consideration of system operation modes and operation targets. *IEEE Access* **2018**, *6*, 31129–31140. [CrossRef]
43. XM SA EPS. En Colombia Factor de emisión de CO2 por generación eléctrica del Sistema Interconectado: 164.38 gramos de CO2 por kilovatio hora, Colombia. Available online: https://www.xm.com.co/noticias/en-colombia-factor-de-emision-de-co2-por-generacion-electrica-del-sistema-interconectado (accessed on 21 September 2022).
44. Academia Colombiana de Ciencias Exactas, F. Factores de Emisión de los Combustibles Colombianos, Colombia, 2016. Available online: https://bdigital.upme.gov.co/bitstream/handle/001/1285/17%20Factores%20de%20emision%20de%20combustibles.pdf;jsessionid=5016BD31B13035A5FBF551BC26B1293E?sequence=18 (accessed on 21 September 2022).
45. Abou El Ela, A.; El-Sehiemy, R.A.; Shaheen, A.; Shalaby, A. Application of the crow search algorithm for economic environmental dispatch. In Proceedings of the 2017 Nineteenth International Middle East Power Systems Conference (MEPCON), IEEE, Cairo, Egypt, 19–21 December 2017; pp. 78–83.
46. Verma, S.; Shiva, C.K. A novel salp swarm algorithm for expansion planning with security constraints. *Iran. J. Sci. Technol. Trans. Electr. Eng.* **2020**, *44*, 1335–1344. [CrossRef]

Disclaimer/Publisher's Note: The statements, opinions and data contained in all publications are solely those of the individual author(s) and contributor(s) and not of MDPI and/or the editor(s). MDPI and/or the editor(s) disclaim responsibility for any injury to people or property resulting from any ideas, methods, instructions or products referred to in the content.